Coded Excitation with Directivity Correction in Synthetic Aperture Imaging System

Ihor Trots, Yuriy Tasinkevych, and Andrzej Nowicki

Abstract The paper presents the preliminary results of the computer simulations of the synthetic aperture method combined with the coded transmission in a linear transducer array. It exploits the transmission of long waveforms characterized by a particular autocorrelation function and allows to increase the total energy of the transmitted signal by its extension, without increasing the peak pressure (limited by safety reasons). It can also improve signal-to-noise ratio and increase the visualization depth maintaining the ultrasound image resolution.

In the computer simulations the 128-element linear transducer array with 0.48 mm inter-element spacing and the 8 and 16-bits Golay sequences as transmission coded signals were used. For comparison a short burst pulse of the half-sine form was also used. The wire phantom with attenuation of 0.5 dB/[MHz $\times$ cm] comprised of several groups of reflectors at different depths was applied. Single element transmission aperture was used to generate a spherical wave covering the full image region and all the elements receive the echo signals. The comparison of 2D ultrasound images of wire phantom is presented to demonstrate the benefits of coded transmission. The visualization was performed using earlier developed synthetic transmit aperture (STA) algorithm with transmit and receive signals correction based on a single element directivity function implemented into the standard STA algorithm.

Keywords Ultrasound imaging • Synthetic aperture • Beamforming • Radiation pattern • Coded sequences • Golay codes

I. Trots (✉) • A. Nowicki
Department of Ultrasound, Institute of Fundamental Technological Research, Polish Academy of Sciences, Pawinskiego 5B, 02-106 Warsaw, Poland
e-mail: igortr@ippt.gov.pl

Y. Tasinkevych
Department of Physical Acoustics, Institute of Fundamental Technological Research, Polish Academy of Sciences, Pawinskiego 5B, 02-106 Warsaw, Poland

A. Nowicki et al. (eds.), *Acoustical Imaging*, Acoustical Imaging 31,
DOI 10.1007/978-94-007-2619-2_16,

1 Introduction

Medical ultrasound imaging is a technique that has become much more prevalent than other medical imaging techniques since it is more accessible, less expensive, safe, simpler to use and produces images in the real time. However, images produced by an ultrasound imaging system, must be of sufficient quality to provide accurate clinical interpretation. The most commonly used image quality measures are spatial resolution and image contrast which can be determined in terms of beam characteristics of an imaging system: beam width and side-lobe level. In the design of an imaging system, the optimal set of system parameters is usually found as a trade-off between the lowest side-lobe peak and the narrowest beam of an imaging system.

In conventional ultrasound imaging system, when one transducer (in mechanical wobble) or linear array are used, the quality of images directly depends on the transducer acoustic field. Also in conventional ultrasound imaging the image is acquired sequentially one image line at a time that puts a strict limit on the frame rate that is important in real-time imaging system. Low frame rate means that moving structures (e.g. heart valves) are not easily imaged and diagnosis may be impaired. This limitation can be reduced by employing synthetic aperture (SA) imaging. The basic idea of the SA method is to combine information from emissions close to each other. The synthetic aperture method has previously not been used in medical imaging. This method is a contrast to the conventional beamforming, where only one image line is created during a transmission. In SA imaging method low resolution images which are obtained, one at a time during a number of transmissions, are summed up to create one high resolution image.

Another crucial factor for image quality in ultrasound imaging is decreasing of the signal-to-noise ratio (SNR) with depth. The severe attenuation of the ultrasonic signals in the tissue results in echoes from large depths literally buried in noise. To overcome this problem, the long wide band transmitting sequences and compression techniques on the receiver side can be applied. The average transmitted power increases proportionally to the length of the code. There are several papers in literature concerning similar boundary-condition problem of signal compression in medical diagnostic imaging [1, 2].

Till now, in SA methods it is assumed that the transmit and receive elements are the point-like sources and the dynamical focusing is realized by finding the geometric distance from the transmitting element to the imaging point and back to the receiving element. But when the element size is comparable to the wavelength the influence of the element directivity on the wave field generation and reception become significant and if ignored might be a source of errors and noise artefacts in the resulting image. In this paper the STA algorithm, which takes into account the single element directivity to improve the quality of the resulting image, is investigated. For this purpose the array element is modeled as a narrow strip transducer with a time harmonic uniform pressure distribution over its width for the far-field radiation pattern calculation. An analytical expression for the corresponding directivity function is available in literature [3]. The far-field assumption is shown to

be acceptable in the considered cases of the transducer dimension to wavelength ratios. As a result the comparison of computer simulation images of the wire phantom obtained for short pulse and Golay complementary sequences used *Field II* simulation program [4] for Matlab environment are presented. The applied coded sequences increased the visualization depth maintaining high image resolution.

2 Synthetic Transmit Aperture Method

As an alternate to the conventional phased array imaging technique the synthetic transmit aperture (STA) method can be used [5, 6]. It provides the full dynamic focusing, both in transmit and receive modes, yielding the highest imaging quality. In the STA method at each time one array element transmits a pulse and all elements receive the echo signals, (see Fig. 1) where data are acquired simultaneously from all directions over a number of emissions, and the full image can be reconstructed from these data. The advantage of this approach is that a full dynamic focusing can be applied to the transmission and the receiving, giving the highest quality of image.

The simple model for the STA ultrasound imaging is given in Fig. 2. In transmission only a single element is used. It creates a cylindrical wave (in the elevation plane the shape of the wavefront is determined by the height of the transducer) which covers the whole region of interest. The received echo comes from all imaging directions, and the received signals can be used to create a whole image – in other words all of the scan lines can be beamformed in parallel. The created image has low resolution because there is no focusing in transmit, and therefore in the rest of this report it is called a low-resolution image. After the first low-resolution image, is acquired another element transmits and a second low-resolution image is created. After all of the transducer elements have transmitted, the low resolution images are summed and a high-resolution image is created.

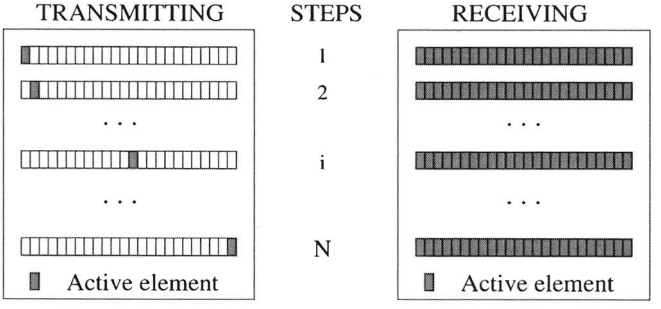

Fig. 1 Transmitting and receiving in STA method

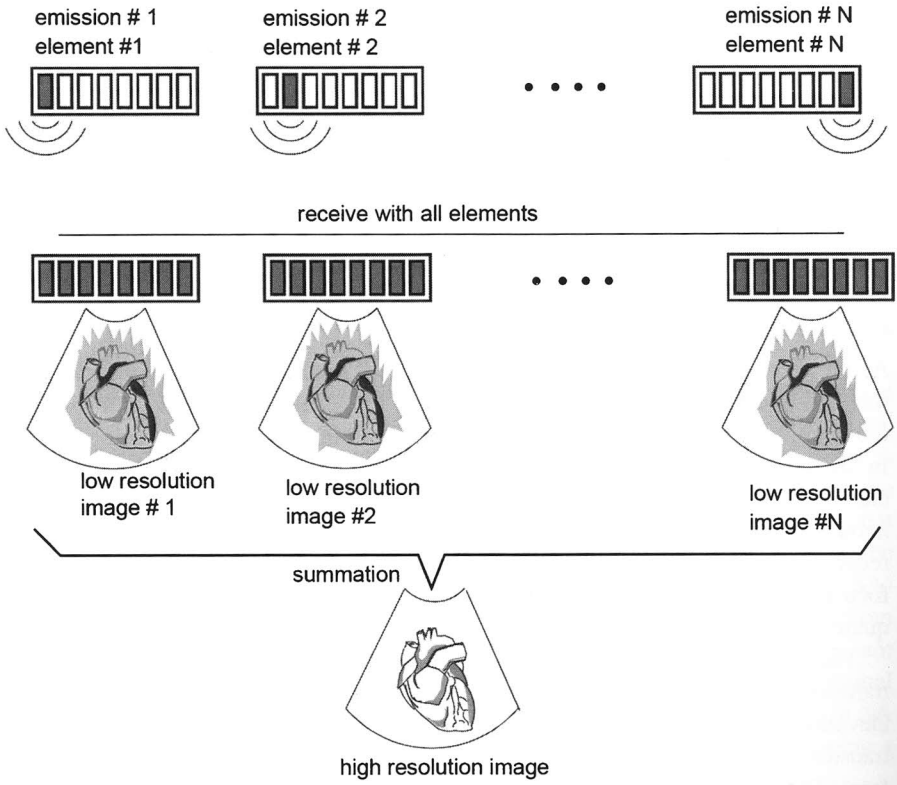

Fig. 2 Low resolution images combined to produce a high resolution image [7]

3 Element Directivity Diagram Influence

In the SA ultrasound imaging methods for each point in the resulting image every combination of transmit-receive pairs contributes according to the round-trip propagation time only. The angular dependence is not taken into account in the applied point-like source model. But when the width of the array element is comparable to the wavelength corresponding to the nominal frequency of the emitted signal, the point-like source model becomes inaccurate. Here, a modified STA imaging algorithm, which accounts for the element directivity function (Fig. 3) and its influence is developed [8].

The underlying idea can be illustrated on the following example, shown in Fig. 4. Here, it is assumed, that the same element transmits and receives signal. Two scatterers located at the points with polar coordinates (r_i, θ_i), $i = 1, 2$ such that $r_{1m} = r_{2m}$ would contribute to the corresponding echo signal $y_{m,m}(t)$ simultaneously, since the round-trip propagation time $2r_{im}/c$, $i = 1, 2$ is the same. Apparently, the contribution from the scatterer at the point (r_1, θ_1) would be dominant, since the observation angle θ_{1m} coincides with the direction of maximum radiation

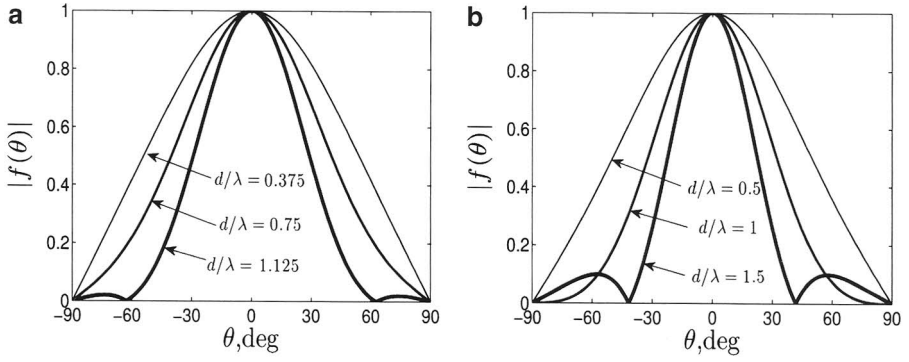

Fig. 3 Directivity function for different values of d/λ

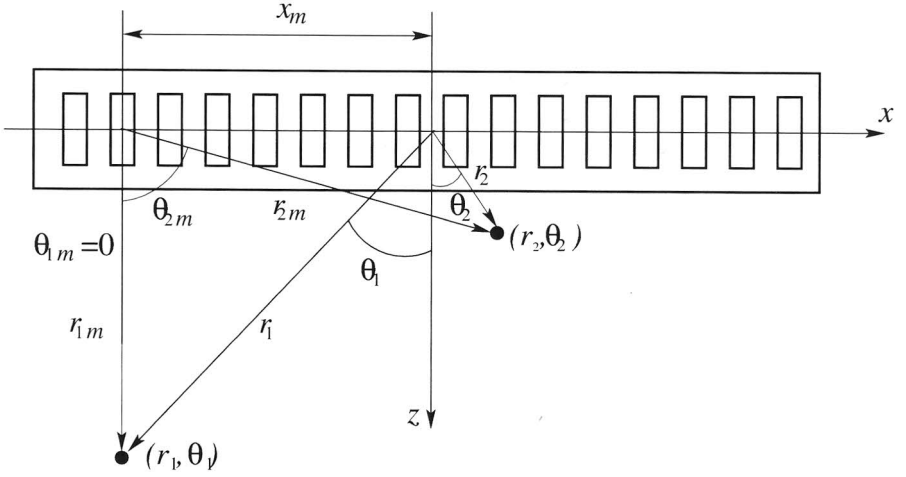

Fig. 4 Influence of the scatterer located at the point (r_1, θ_1) on the value of resulting signal $A(r_2, \theta_2)$ for imaging point (r_2, θ_2)

for the m-th element, whereas its transmit-receive efficiency at the angle θ_{2m} is much smaller for the case of the scatterer at the point (r_2, θ_2). Thereby, evaluating the value of $A(r_2, \theta_2)$ from Eq. 1 (provided that $f(\theta_i) \equiv 1$, i = n, m, is assumed), the partial contribution of the echo $y_{m,m}(t)$, in addition to the correct signal from the obstacle located at (r_2, θ_2) (being small due to the large observation angle θ_{2m}), would also introduce the erroneous signal from the scatterer located at (r_1, θ_1). The latter signal is larger due to the small observation angle θ_{1m}. The larger observation angles appear in the imaging region close to the array aperture. Therefore, the most appreciable deviation from the point-like source model of the array element will occur there. A solution to the problem, which accounts for the observation angle in accordance with the array element directivity function, is proposed. Assume, that the dependence of the transmit-receive efficiency of a single array element versus

the observation angle is known and is denoted by $f(\theta_m)$, where θ_m is measured from the line parallel to z-axis and passing through the m-th element center. Thus, in order to suppress the erroneous influence from the scatterer located at (r_1, θ_1) on the value of the resulting signal $A(r_2, \theta_2)$, the partial contribution of the echo $y_{m,m}(t)$ is weighted by the corresponding value of $f(\theta_{2m})$. This corresponds to the superposed signal correction in accordance with respective contributions of individual scatterers located at the points (r_1, θ_1) and (r_2, θ_2).

The above considerations lead to the following modification of the synthetic focusing imaging algorithm

$$A(r,\theta) = \sum_{m=1}^{N}\sum_{n=1}^{N} f(\theta_m) f(\theta_n) y_{m,n}\left(\frac{2r}{c} - \tau_{m,n}\right), \tag{1}$$

where $\theta_i(r, \theta)$, $i = m, n$ are the corresponding observation angles for the transmit-receive pair. The modification of the STA thus is expressed by a weighted summation of properly delayed RF signals (as in the case of conventional STA). The corresponding weights $f(\theta_m), f(\theta_n)$ in the transmit and receive modes are calculated by means of the single element directivity function. Note, that the angles depend on the spatial location of the imaging point (r, θ). The directivity function $f(\theta)$ can be calculated in the far-field approximation for a single element of the array transducer in analogous manner as in [3] (see example in Fig. 3)

$$f(\theta) = \frac{\sin(\pi d/\lambda \sin\theta)}{\pi d/\lambda \sin\theta} \cos\theta, \tag{2}$$

where d is the element width, and λ is the wavelength. Some examples of the directivity function evaluated for different values of the ratio d/λ are shown in Fig. 3. Note, in Fig. 3b the values of d/λ correspond to the case when the element width d = 0.75*pitch, and the pitch is 0.5, 1, and 1.5 of the lambda, respectively. The above result applies to a narrow strip transducer with a time harmonic uniform pressure distribution along its width. It is obtained by means of the Rayleigh-Sommerfeld formula in the far-field region. For simplicity, Eq. 2 is applied in the numerical results presented in the next section. It should be noted, that the angular response $f(\theta)$ in Eq. 1 evaluated from Eq. 2 for some fixed value of λ, which corresponds to the nominal frequency of the transmitted signal was used.

4 Coded Excitation: Golay Complementary Sequences

Among the different excitation sequences proposed in ultrasonography, Golay codes evoke more and more interest in comparison with other signals. The reason of that lies in the fact that Golay codes, like no other signals, suppress to zero the amplitude of side-lobes. This type of complementary sequences has been

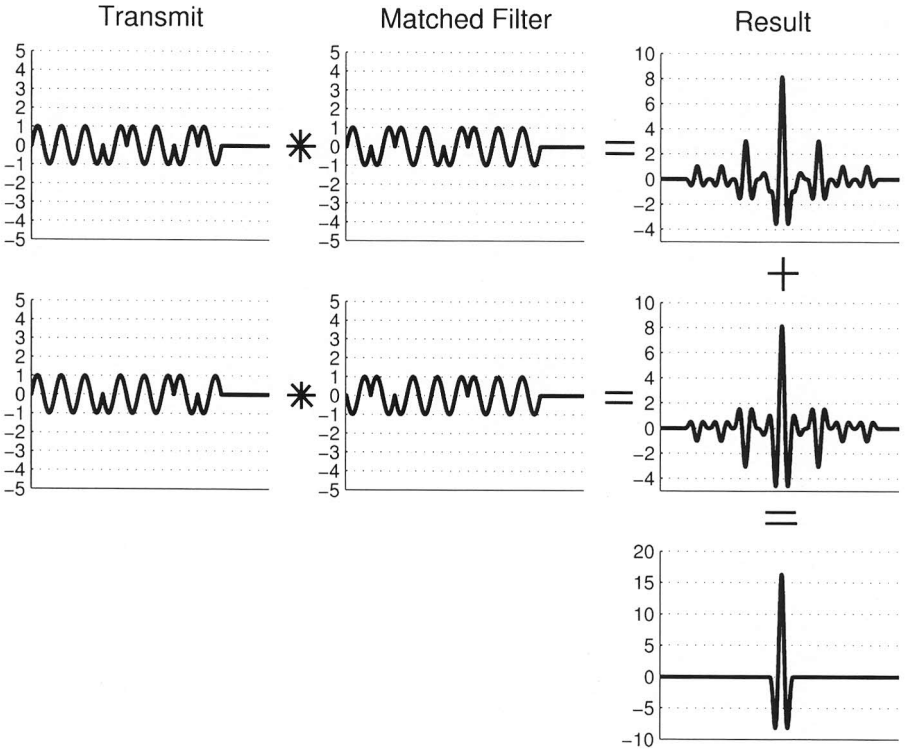

Fig. 5 Principle of side-lobes cancellation using pair of Golay complementary sequences of length 8 bits

introduced by Golay [9, 10]. The pairs of Golay codes belong to a bigger family of signals, which consist of two binary sequences of the same length n, whose auto-correlation functions have the side-lobes equal in magnitude but opposite in sign. The sum of these auto-correlation functions gives a single auto-correlation function with the peak of $2n$ and zero elsewhere [11].

Figure 5 shows the pair of complementary Golay sequences, their auto-correlations, and the zero side-lobes sum of their autocorrelations.

As can be seen from the Fig. 5, the key to side-lobes canceling property of Golay code pairs is that the range side-lobes of one are equal in amplitude and opposite in sign to the side-lobes of the other.

5 Computer Simulation and Discussion

Simulation is a fundamental way of testing methods. This is done to confirm or reject a hypothesis in a controlled environment. Since it is possible to control all parameters in a simulation, one can set up a simple model and then gradually

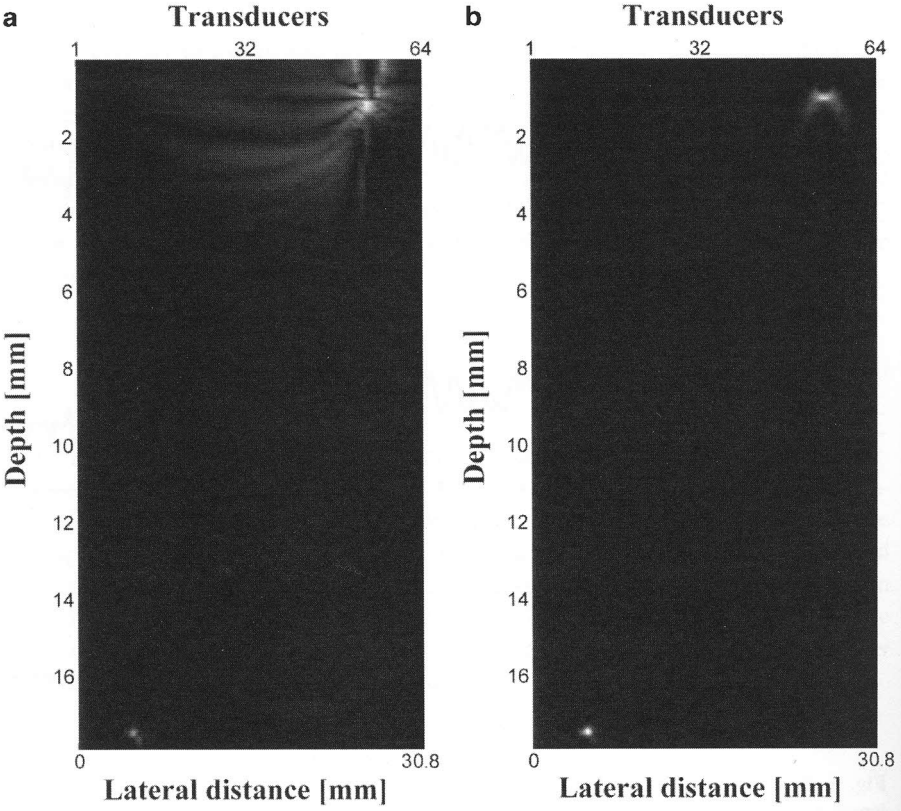

Fig. 6 Simulation of 2 point scatterers for 64-element linear array: (**a**) not including directional diagram of element; (**b**) including directional diagram of element

transform it into something more similar to reality. When this is done one can continue with measurements and confirm or reject the simulations for a real setup, in vivo or on a phantom. All simulations in this work are carried out with a powerful software, *Field II*. The program is developed especially for investigating ultrasound fields, and gives the possibility to simulate and calculate ultrasound fields and defining one's own transducer. *Field II* runs under Matlab and the accuracy is very high since *Field II* is based on numerical analysis.

The numerical results presented in Fig. 6 were performed for a 64-element linear transducer array excited by one sine cycle burst pulse at a nominal frequency of 5 MHz. The element pitch is 1.5λ, where λ corresponds to the nominal frequency of the burst pulse. The STA algorithm is employed. The transmit and receive elements combinations give a total of 64×64 possible RF A-lines. All these A-lines echo signals are sampled independently at a frequency of 50 MHz and stored in RAM.

In Fig. 7 a computer simulation of multi-scatterers phantom when a 128-element linear transducer array with 0.48 mm inter-element spacing was applied is shown.

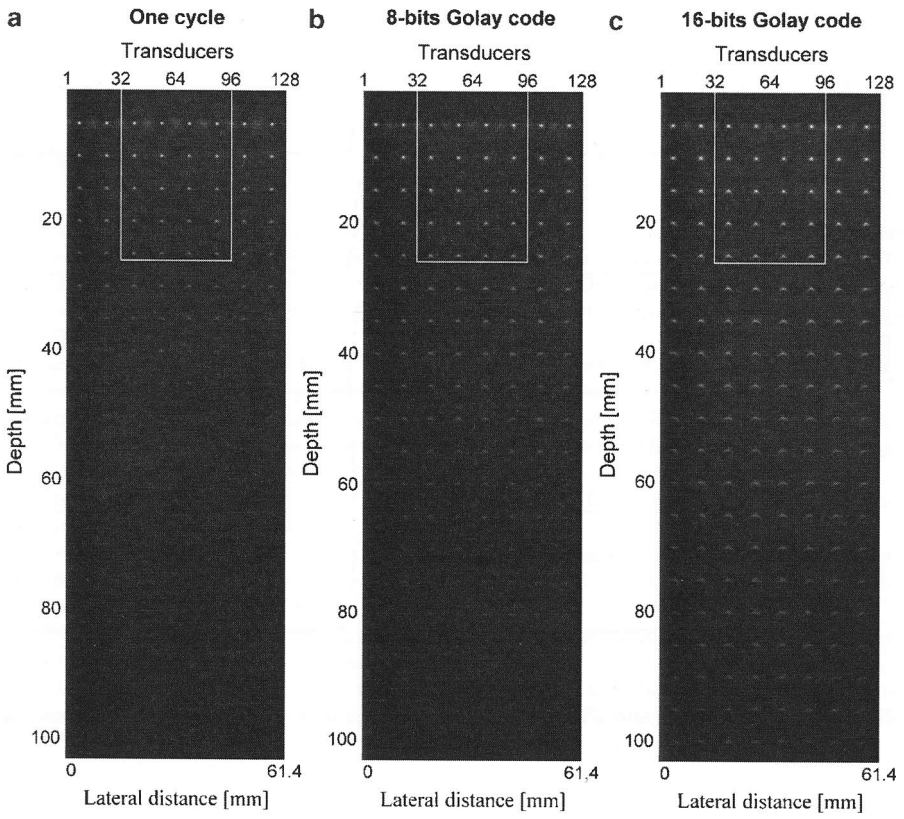

Fig. 7 Comparison of 2D ultrasound images obtained by computer simulation for 128-element linear array using: (**a**) one cycle; (**b**) 8-bits Golay sequences; (**c**) 16-bits Golay sequences. The phantom attenuation is equal to 0.5 dB/[MHz × cm]

The one cycle as well as the pairs of complementary Golay sequences of the lengths 8 and 16 bits at nominal frequency 5 MHz were used. The phantom attenuation is equal to 0.5 dB/[MHz × cm].

The obtained 2D ultrasound images clearly demonstrate the advantage of using the Golay coded sequences. With the elongation of the coded sequences the acoustical power increases yielding a higher SNR, that leads to an increase in the penetration depth while maintaining both axial and lateral resolution. The latter depends on transducer acoustic field and is discussed in [12]. The visualization depth when the one cycle was applied is equal to 3 cm (Fig. 7a), while in case of applying 8-bits Golay codes this depth increases to 5 cm (Fig. 7b), and for longer 16-bits Golay codes this depth of visualization increases up to 8 cm (Fig. 7c).

In order to compare the lateral resolution the cross section of phantom marked by rectangular in Fig. 7 is shown in Fig. 8.

Figure 8 shows that the lateral resolution for different burst signals is the same.

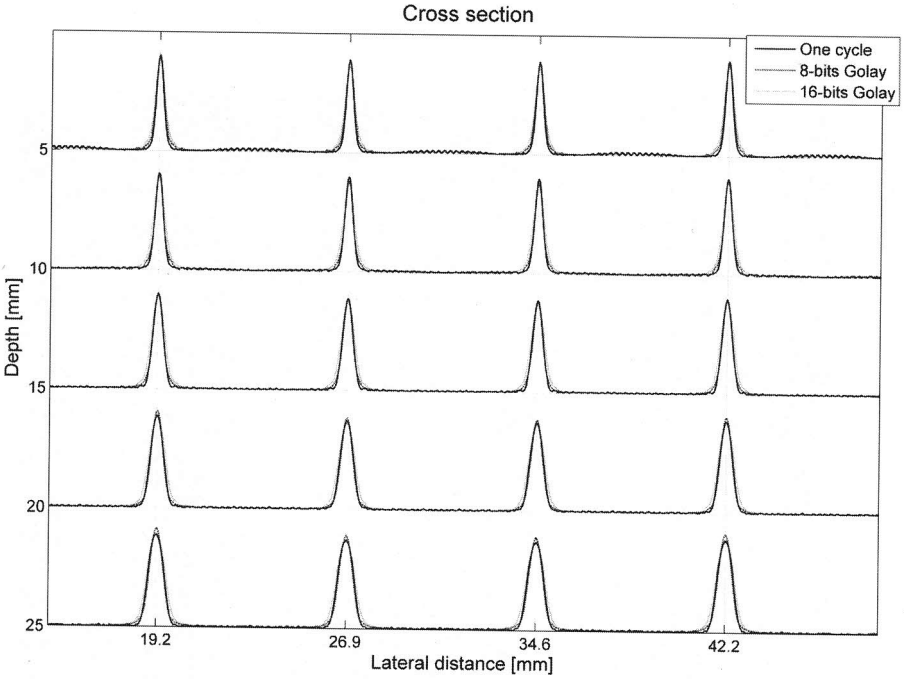

Fig. 8 Comparison of the lateral resolution at different depths: 5, 10, 15, 20 and 25 mm when one cycle, 8 and 16-bits Golay sequences were applied

6 Conclusions

The new algorithm based on the array element angular directivity function implementation into the conventional STA method and corresponding correction of the back-scattered RF signals of different transmit-receive pairs is presented. It is shown that the far-field radiation pattern of a narrow strip transducer, calculated for the case of a time harmonic uniform pressure distribution over its width, can serve as a good approximation for the above directivity function. The results of numerical calculations using simulated data have shown distinguishable improvement of the imaging quality of the scatterers situated in the region near the transducer aperture, the hazy blurring artefacts, observable in the case of conventional STA algorithm, are substantially suppressed.

Also the coded transmission in STA method is discussed. The main advantage of the coded transmission is increasing of the transmission energy that in its turn allows to improve the penetration depth and makes the ultrasound image more contrast. The comparison of the 2D ultrasound images show that elongated coded sequences from 8-bits to 16-bits increase the penetration depth by about 2 cm. Applying of the coded transmission in the STA method in a standard ultrasound scanner could allow to increase the efficiency and quality of the ultrasound diagnostic.

Acknowledgments This work was supported by the Polish Ministry of Science and Higher Education (Grant NN518382137).

References

1. Nowicki, A., Secomski, W., Litniewski, J., Trots, I.: On the application of signal compression using Golay's codes sequences in ultrasound diagnostic. Arch. Acoust. **28**(4), 313–324 (2003)
2. Klimonda, Z., Lewandowski, M., Nowicki, A., Trots, I.: Direct and post-compressed sound fields for different coded excitations – experimental results. Arch. Acoust. **30**(4), 507–514 (2005)
3. Selfridge, A.R., Kino, G.S., Khuri-Yakub, B.T.: A theory for the radiation pattern of a narrow-strip acoustic transducer. Appl. Phys. Lett. **37**(1), 35–36 (1980)
4. Jensen, J.A.: Field: a program for simulating ultrasound systems. Paper presented at the 10th Nordic-Baltic conference on Biomedical Imaging Published in Medical & Biological Engineering & Computing. **34**(Suppl. 1, Part 1), 351–353 (1996)
5. Jensen, J.A., Nikolov, S.I., Gammelmark, K. L., Pedersen, M.H.: Synthetic aperture ultrasound imaging. Ultrasonics **44**, e5–e15 (2006)
6. Trahey, G.E., Nock, L.F.: Synthetic receive aperture imaging with phase correction for motion and for tissue ihomogeneities – part I: basic principles. IEEE Trans. Ultrason. Ferroelectr. Freq. Control **39**(4), 489–495 (1992)
7. Nikolov, S.I.: Synthetic aperture tissue and flow ultrasound imaging. PhD thesis, Technical University of Denmark (2001)
8. Tasinkevych, Y., Nowicki, A., Trots, I.: Element directivity influence in the synthetic focusing algorithm for ultrasound imaging. In Proceedings of the 57th Open Seminar on Acoustics (OSA 2010), pp. 197–200, Gliwice (2010)
9. Golay, M.J.E.: Complementary series. IRE Trans. Inform. Theory **IT-7**, 82–87 (1961)
10. Golay, M.J.E.: Multislit spectrometry. J. Opt. Soc. Am. **39**, 437–444 (1949)
11. Trots, I., Nowicki, A., Secomski, W., Litniewski, J.: Golay sequences – side-lobe canceling codes for ultrasonography. Arch. Acoust. **29**(1), 87–97 (2004)
12. Nowicki, A., Klimonda, Z., Lewandowski, M., Litniewski, J., Lewin, P.A., Trots, I.: Direct and post-compressed sound fields for different coded excitation. Acoust. Imaging **28**(5), 399–407 (2007)